Journal of Physics:
Conference Series

PAPER • OPEN ACCESS

Adsorption and kinetic studies of dyes onto $BaFe_{12}O_{19}$ Ferrite Nanoparticles

To cite this article: N. A. Erfan and A. A. Mohammed 2024 *J. Phys.: Conf. Ser.* **2830** 012016

Adsorption and kinetic studies of dyes onto $BaFe_{12}O_{19}$ Ferrite Nanoparticles

N. A. Erfan[1] and A. A. Mohammed[1]

[1] Chemical engineering department, faculty of engineering, Minia university, Minia, Egypt.

n.erfan1@mu.edu.eg

Abstract. In this work, Barium hexaferrite ($BaFe_{12}O_{19}$) nanoparticles were used for industrial waste water treatment from methylene blue (MB) and congored (CR) dyes. Batch adsorber with mechanical stirring column was used to test various experimental parameters like contact time, initial dye concentration and adsorbent dosage for the removal of these dyes. For the removal of MB and CR dyes using magnetic nanoparticles, the maximum adsorption capacities were 200 and 124.5 mg/g respectively. The maximum removal efficiencies were 90 % for MB removal onto the nanoparticles and 80% for CR removal. In order to analyze the kinetic data, pseudo first and second order kinetic models have been used. For all studied variables and based on correlation coefficient (R) values and graphical presentation, the results confirm that pseudo second order model fits well the experimental data.

Key words: Adsorption; removal; Ba-hexaferrite; nanoparticles; Methylene blue; Congo red

1. Introduction

The rapid industrialization development and growth of population made the contamination of surface and ground water a worldwide critical problem [1-3]. Therefore, it's essential to control the contaminants harmful effects [4,5]. The major contaminants of waste water are heavy metals besides organic and inorganic pollutants. The use of synthetic dyes in various industries such as pulp and paper, plastics, cloth dyeing, leather treatment and printing increased considerably over the last few years. The toxicity of some of these dyes in nature made their removal through waste water a severe problem to human beings and ecological environment [6]. Rapid significant progresses in waste water treatment including bioremediation, photocatalytic oxidation and adsorption/separation processing were made in order to face the water pollution problem [7]. However, processing efficiency, operational methods, energy requirements and economic benefits are the factors restricted their applications. Among these methods, adsorption can be considered as the economical and efficient alternative for dyes removal from aqueous solutions. From the stand point of both resource conservation and environmental remediation, magnetic materials have been recently suggested as efficient, economic alternative to existing treatment materials. The most Egyptian localities rich with iron ore mines are Eastern desert, East Aswan, Baharyia oasis and Western desrt. Iron ore in these localities widely varies in their mineralogical and chemical composition. Reaching the suitable size for blast furnace burden needs accurate pretreatment for the extracted iron ore where huge number of ore (about 20%) is wasted. Magnetic glass ceramic material was prepared in this work using Bahariya oasis ore which contains 51% pure iron. Different methods for magnetic nanoparticles synthesis have been used by previous workers such as sol-gel, co-precipitation, electrochemical method, hydrothermal method, sonochemical and mechanical methods. For example, Comanescu et. Al. [8] prepared magnetic nanoparticles by using size-cotrolling agent such as Polyethyleneimine (PEI), which act effectively as surface coat, Tetiana Tatarchuk et al. [9] synthesized Fe_3O_4 nanoparticles by the co-precipitation method. Among the various synthesis methods mechanical method is the simpler and cost effective. In this study, in order to convert the bulk magnetic glass ceramics into nanosize (MGNPS) mechanical method using high energy ball milling technique was used. The capacity of treating large amount of waste water within short time and easy separation are the main advantages of using magnetic nanoparticles. To the best of our knowledge, it is the first time to use Baharyia oasis iron ore for producing magnetic glass ceramic nanoparticles. Furthermore, the novelty of this work is obvious in studying the kinetics during the adsorption of dyes from aqueous solution in mechanical stirring batch adsorber using the produced nanoparticles.

2. Experimental methods

The composition of the MGNPS is ~37% iron ore waste in addition to Na_2CO_3, $NH_4H_2PO_4$, $BaCO_3$, H_3BO_3 and TiO_2 as a source for Na_2O, P_2O_5, BaO, B_2O_3 and TiO_2 respectively. The required amounts of chemicals were melted at 1200 ºC for 2 h with occasional swirling every 30 min using a platinum crucible. At room temperature the melts were poured onto a stainless-steel plate and pressed to 1-2 mm thick strips by another cold steel plate. The strips were heat treated at 900ºC for 2 h. A desktop high speed vibrating ball mill was used at room temperature to produce magnetic nanoparticles. The experimental work including water treatment experiments have discussed in detail in previous work [10].

3. Results and discussions

The conversion to nanosize after 5 h milling has been confirmed from figure 1A (SEM) and 1B (TEM) as uniformly distributed very fine particles were detected. Using image j program, the particles average size after 5h milling duration were measured to be 26 nm. Figure 1C depict XRD result for the MGNPS where Ba-hexaferrite ($BaFe_{12}O_{12}$) crystallization as matching ASTM card No84-0757 was confirmed. Figure 1 D shows the room temperature magnetic hysteresis (*M-H*) loops of the MGNPS of under a magnetic field strength of 20 KOe. The particles saturation magnetization (21.18 emu/g) is an indication for Ba-hexaferrite as a ferromagnetic phase crystallization, the coercivity was measured to be 1550 Oe. It can be observed from the loops that *Mr/Ms* value is 9.32. This remanence ratio was due to the increasing percentage of fractured particles and the formation of most of the nanoparticles with increasing milling time as confirmed by XRD results.

In this work, Congored (CR) and methylene blue (MB) were used to study the magnetic nanoparticles (MGNPS) removal capacity. The following equation qe = (Co − Ce) V m has been used to calculate the amount of adsorbed dye, where Co and Ce are the initial and final concentration of dye (mg/l) respectively, qe is the adsorbent capacity at equilibrium, V the dye solution volume and m is the adsorbent mass (g). Methylene blue (MB) and congo red (CR) dyes adsorption by MGNPS as a function of equilibrium concentration is shown in figure 2 where q_e value was reached after 17 and 8 mins respectively. Initially, the dye adsorption was quite rapid and with time the rate of adsorption became slower before reaching constant value (equilibrium time). Uncovered adsorbent surface area in addition to the electrostatic attraction between particles surface and the dyes is the reason for the initial faster rate. MGNPS adsorption capacity for MB and CR is 95 and 124 mg/g respectively. A comparison between the theoretical and experimental MB and CR adsorption isotherm is represented in figure 3. Standard deviation (SD) values were used to show the level of fitting of each model. The greater the precision between theoretical and experimental q values is confirmed by lower SD value. Therefore, the theoretical fits the experimental data for MB and CR dyes sorption on MGNPS.

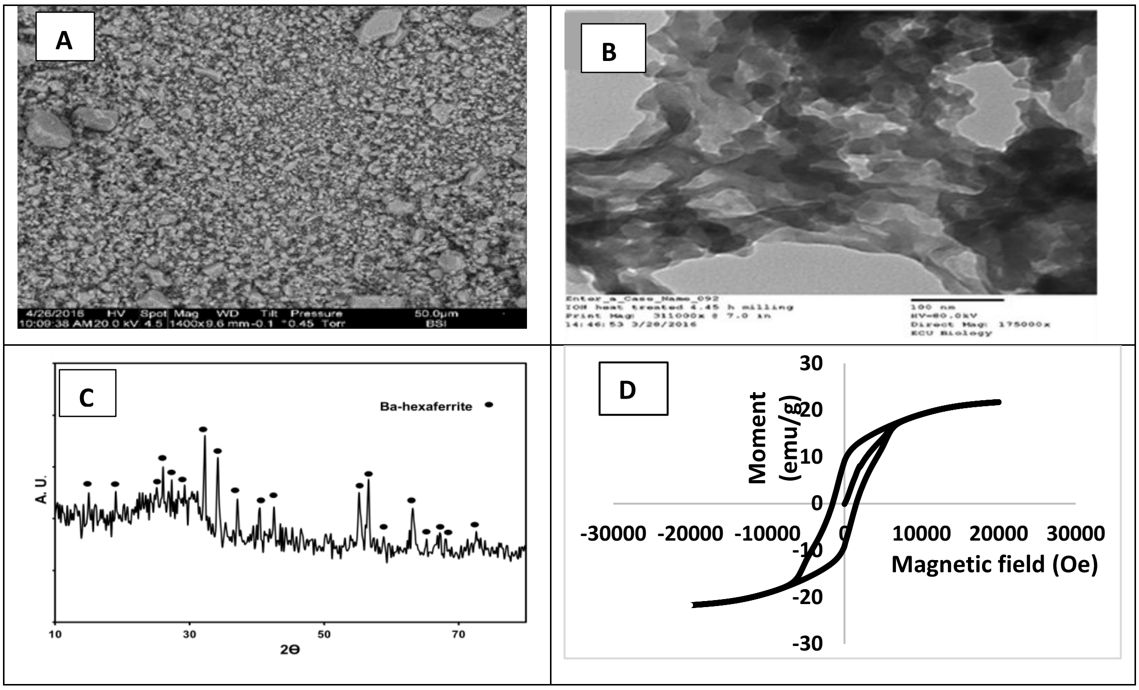

Figure 1. (A) Sem image, (B) TEM image, (C) XRD, and (D) Room temperature M-H hysteresis loop of MGNPS.

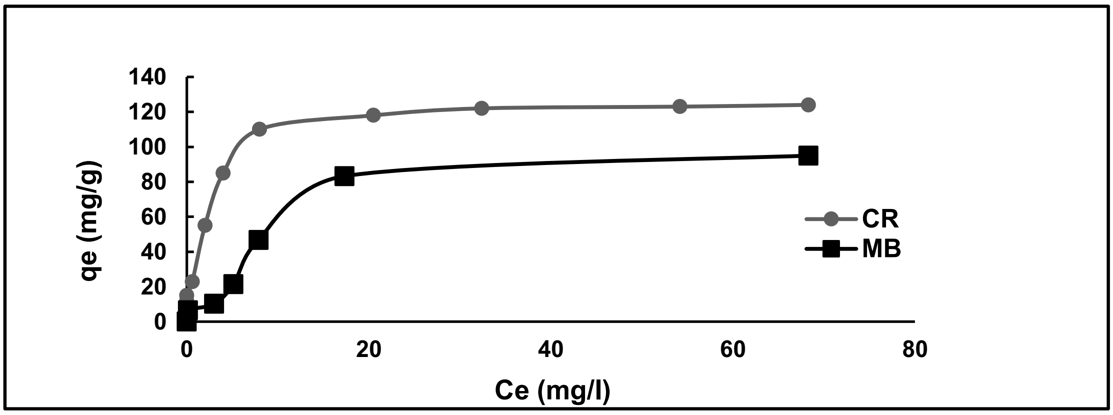

Figure 2. Adsorption of CR and MB onto magnetic nanoparticles as a function of equilibrium concentration.

The Lagergern pseudo 1st order model confirms that the adsorption capacity depends on the rate of adsorption of solute on adsorbent. The nonlinear form of pseudo 1st order equation is presented in equation 1:

$$\frac{dqt}{dt} = k_1 (q_1\text{-}q_t) \qquad (1)$$

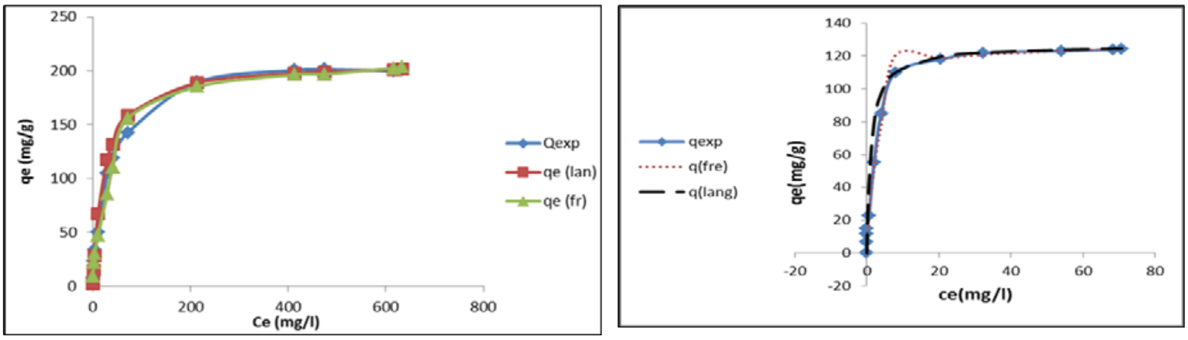

Figure 3. Comparison between experimental and theoretical isotherm for the adsorption of (A) MB and (B) CR onto the MGNPS.

As shown in equation 2, the integrated rate law became a linear equation at initial conditions of q_t=0 at t=0

$$\text{Log } (q_1\text{-}q_t) = \log q_1 - \frac{k1}{2.3033} t \qquad (2)$$

K_1 is the rate constant for pseudo 1st order (min^{-1}), q_1 is the quantity of adsorbate that is divided by the amount of adsorbent which is present at equilibrium (mg/g), and q_t is the adsorption capacity that is present at any time (mg/g). q_1 and k_1 can be calculated from the slope and the intercept by plotting Log (q_1-q_t) versus t (slope = k_1, q_1 = exp intercept). The linear plots of the first order kinetic model as Log (q_1-q_t) versus time for the adsorption of MB on MGNPS at different agitation speeds, initial dye concentration and MGNPS mass were investigated in figure 4. The slopes and intercepts of these linear plots are used to determine the pseudo first order rate constant (k1), the amount of dye adsorbed at equilibrium (q1), and correlation constant (R_1^2) which are reported in table (1). There's a significant deviation from the straight lines of the pseudo first order kinetics over the entire range of the adsorption period as shown in figure (4). The values of the coefficient of determination (R_1^2) for the linear plots are relatively low (0.9-.97) as shown in table 1. At all variables the values of the theoretical equilibrium adsorption capacity (q_1) were found to be lower than the values obtained experimentally (q_{exp}). This suggests that the adsorption of MB on the MNP doesn't follow the pseudo first order kinetics.

The pseudo 2nd order kinetic model is shown in equation (3) as follow:

$$\frac{t}{qt} = \frac{1}{k2\ q2\ 2} + \left(\frac{1}{q2}\right) t \qquad (3)$$

K_2 (g/mg.min) is a rate constant for pseudo 2nd order adsorption, q_2 is the quantity of adsorbate divided by the adsorbent at equilibrium (mg/g), and qt is the quantity of adsorbate divided by the adsorbent at any time (mg/g).

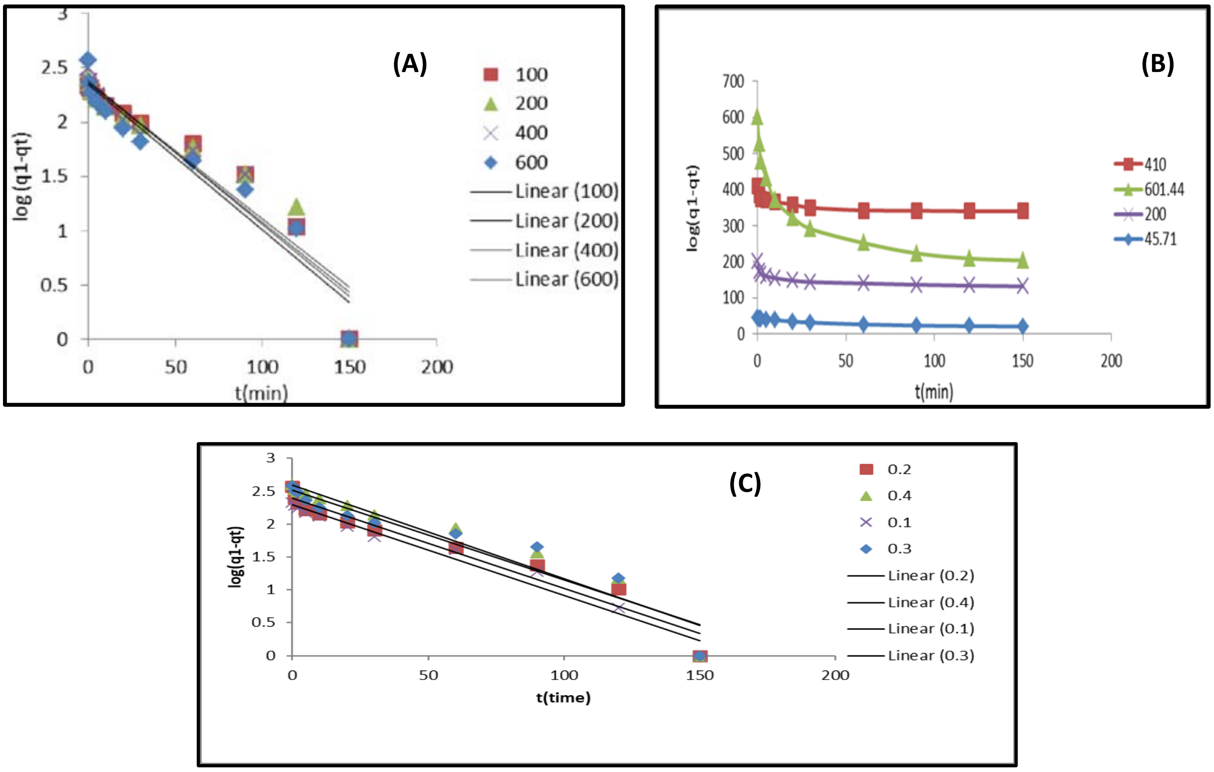

Figure 4. Lagergren pseudo first order kinetics for adsorption of MB at different [A] agitation speeds (100-600 rpm), [B] Initial dye concentration (45-600 mg/l) and [C] MGNPS mass (0.1-0.4 g).

By plotting t/qt versus t, q_2 and k_2 can be calculated from the slope and intercept. The initial rate of sorption h (mg/g.min) at t=0 was calculated using K_2 constant as shown in equation (4):

$$h = K_2\, q_2^2 \qquad (4)$$

Agitation speed, initial MB dye concentration and MGNPS mass were the parameters taken into consideration to investigate the second order model. Mb adsorption onto the MGNPS at different agitations speeds, initial dye concentration and MGNPS mass was depicted in figure 5. As presented in table 2 the calculated values of q_2 were very close to the experimental results q_{exp}. The coefficient R^2 values ranging from 0.9 to 0.99. The results as indicated from figure 5 and table 2 confirms that MB adsorption onto the MGNPS followes a pseudo second order kinetic model.

4. Adsorption mechanism

Adsorption take place when the net force acting on the particle on the surface and bulk of adsorbent are not the same. dyes have unbalanced forces acting on them which are called residual attractive forces. During the adsorption process, charge transfer take place between the dye molecules and the MGNPS which results in a dipole moment . Therefore, the dye molecules adhere to the surface of the MGNPS and form a film on the MGNPS surface. Further investigation to the heat effect has to be done in order to classify the adsorption process in this work as chemisorption or physiosorption.

Table 1. Pseudo 1st order model parameters values at different variables for MB adsorption onto MGNPS

Variables	Agitation Speed (rpm)				Initial Conc. Co (mg/l)				Mass of adsorbent (g)			
	100	**200**	**400**	**600**	**601**	**410**	**200**	**45.71**	**0.1**	**0.2**	**0.3**	**0.4**
R^2_1	0.9	0.9	0.9	0.9	0.94	0.92	0.9	0.9	0.97	0.945	0.911	0.923
q_{exp} (mg.g^{-1})	217.4	255.44	315.22	370	397.87	380.43	369.57	24.57	209.8	369.5	383.9	403
q_1 (mg.g^{-1})	231.6	231.526	240.104	220	235	238	245	22	196	245	326	392
k_1 (min^{-1})	0.03	0.03	0.03	0.03	0.04	0.05	0.03	0.02	0.03	0.03	0.03	0.03

Table 2. Pseudo 2nd order model parameters values at different variables for MB adsorption onto MGNPS

Variables	Agitation Speed (rpm)				Initial Conc. Co (mg/l)				Mass of adsorbent (g)			
	100	**200**	**400**	**600**	**601**	**410**	**200**	**45.71**	**0.1**	**0.2**	**0.3**	**0.4**
R^2_1	0.9732	0.9875	0.9935	0.9974	0.934	0.903	0.941	0.923	0.99	0.996	0.992	0.985
q_{exp} (mg.g^{-1})	217.391	255.44	315.22	369.57	397.865	380.435	369.565	24.5699	209.826	383.936	369.565	402.907
h	11.898	24.931	49.805	94.65	98.0903	103.107	77.503	1.573	17.679	77.5034	48.0769	36.2847
q_2 (mg.g^{-1})	232.558	263.16	312.5	370.37	416.667	384.615	370.3704	26.6667	222.222	370.37	384.615	416.667
K_2 (min^{-1})	0.00022	0.0004	0.0005	0.0007	0.00057	0.0007	0.000565	0.00221	0.00036	0.00057	0.00033	0.00021

5. Conclusions

Baharaya oasis ore waste was successfully recycled into hard ferromagnetic glass ceramics and efficient magnetic nanoparticles (MGNPS) were prepared using ball milling technique. The adsorption capacity of the MGNPS were calculated as 95 and 124 mg/g for MB and CR respectively and the mechanism of interaction between adsorbent and adsorbate was investigated. For sorption of MB and CR dyes onto MGNPS, the theoretical fits the experimental data. In the adsorption experimental data, Pseudo 2nd order was proved to be more fitted.

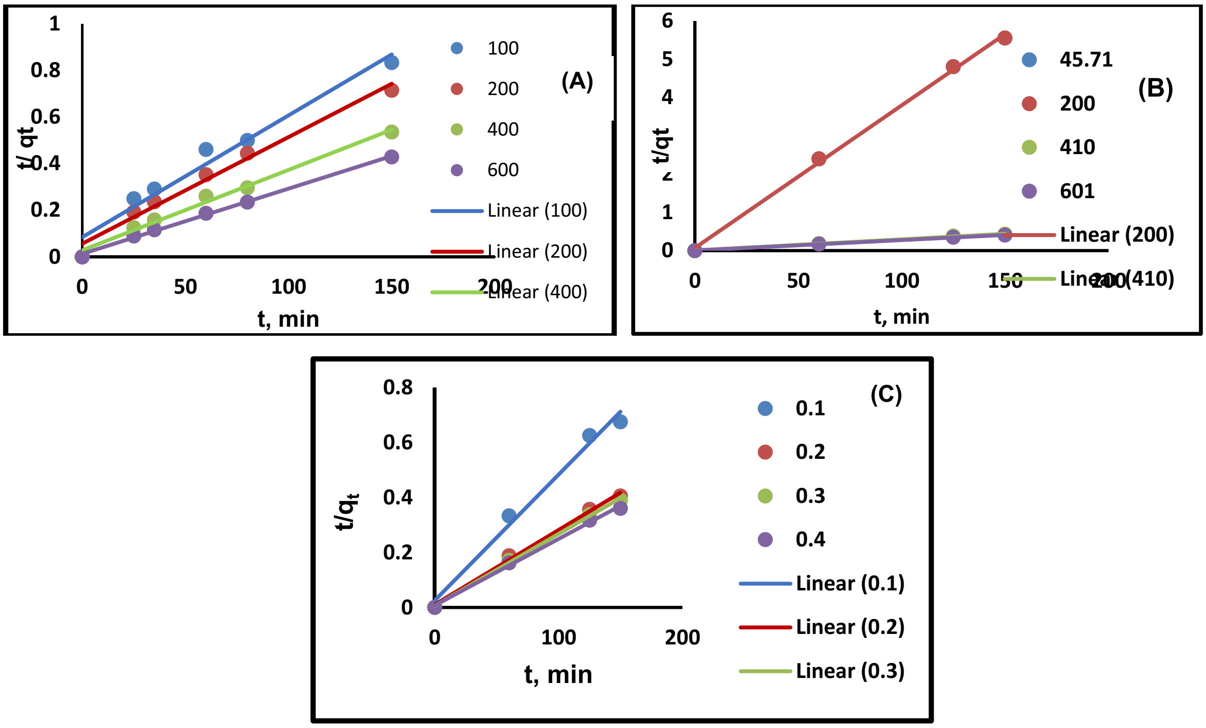

Figure 5. Lagergren pseudo second order kinetics for adsorption of MB at different [A] agitation speeds (100-600 rpm), [B] Initial dye concentration (45-600 mg/l) and [C] MGNPS mass (0.1-0.4 g).

References

[1] Andrew B. Cundy, Laurence Hopkinson, Raymond L. D. Whitby 2008 *Science of The Total Environment* 400 42. https://doi.org/10.1016/j.scitotenv.2008.07.002

[2] Meng Nan Chong, Bojin, Christopher W. K. Chow, Chris Saint 2010 *Water Research* 44 2997. https://doi.org/10.1016/j.watres.2010.02.039

[3] Guangming Zeng, Jiachao Zhang, Yaoning Chen, Zhen Yu, Man Yu, Hui Li, Zhifeng Liu, Ming Chen, Lunhui Lu, Chunxiao Hu 2011 *Bioresource Technology* 102 9026. https://doi.org/10.1016/j.biortech.2011.07.076

[4] D. Fatta-Kassinos, M.I. Vasquez, K. Kümmerer 2011 *Chemosphere* 85 693. https://doi.org/10.1016/j.chemosphere.2011.06.082

[5] Yecong Li, Wenguang Zhou, Bing Hu, Min Min, Paul Chen, Roger R. Ruan 2011 *Bioresource Technology* 102 10861. https://doi.org/10.1016/j.biortech.2011.09.064

[6] Pang, Z., Yang, N., Vierbuchen, T. 2011 *Nature* 476 220.

[7] Grigory Zelmanov, Raphael Semiat 2008 *Water Research* 42 3848. https://doi.org/10.1016/j.watres.2008.05.009

[8] Comanescu C. 2023 *Coatings* 13 1772. https://doi.org/10.3390/coatings13101772

[9] Tetiana Tatarchuk, Nazarii Danyliuk, Ivanna Lapchuk, Alexander Shyichuk, Volodymyr Kotsyubynsky 2022 *Materials Today: Proceedings* 62 5805. https://doi.org/10.1016/j.matpr.2022.03.494

[10] Nehal A. Erfan, Salwa AM Abdel-Hameed, and Asma A. Mohammed 2020 *The International Conference on Chemical and Environmental Engineering Military Technical College* 10 1. https://doi.org/10.1088/1757-899X/975/1/012002.